Protein Science (2000), *9*:242–251. Cambridge University Press. Printed in the USA.
Copyright © 2000 The Protein Society

Characterization of the functional role of Asp141, Asp194, and Asp464 residues in the Mn^{2+}-L-malate binding of pigeon liver malic enzyme

WEI-YUAN CHOU,[1] HWEI-PING CHANG,[1] CHIEN-HSIUN HUANG,[1] CHENG-CHIN KUO,[1] LIANG TONG,[2] AND GU-GANG CHANG[1]

[1]Department of Biochemistry, National Defense Medical Center, Taipei 100, Taiwan, Republic of China
[2]Department of Biological Sciences, Columbia University, New York, New York 10027

(RECEIVED June 8, 1999; FINAL REVISION October 20, 1999; ACCEPTED October 20, 1999)

Abstract

Pigeon liver malic enzyme was inactivated and cleaved at Asp141, Asp194, and Asp464 by the Cu^{2+}-ascorbate system in acidic environment. Site-specific mutagenesis was performed at these putative metal-binding sites. Three point mutants, D141N, D194N, and D464N; three double mutants, D(141,194)N, D(194,464)N, and D(141,464)N; and a triple mutant, D(141,194,464)N; as well as the wild-type malic enzyme (WT) were successfully cloned and expressed in *Escherichia coli* cells. All recombinant enzymes, except the triple mutant, were purified to apparent homogeneity by successive Q-Sepharose and adenosine-2′,5′-bisphosphate-agarose columns. The mutants showed similar apparent $K_{m,NADP}$ values to that of the WT. The $K_{m,Mal}$ value was increased in the D141N and D194N mutants. The $K_{m,Mn}$ value, on the other hand, was increased only in the D141N mutant by 14-fold, corresponding to ~1.6 kcal/mol for the Asp141-Mn^{2+} binding energy. Substrate inhibition by L-malate was only observed in WT, D464N, and D(141,464)N. Initial velocity experiments were performed to derive the various kinetic parameters. The possible interactions between Asp141, Asp194, and Asp464 were analyzed by the double-mutation cycles and triple-mutation box. There are synergistic weakening interactions between Asp141 and Asp194 in the metal binding that impel the D(141,194)N double mutant to an overall specificity constant $[k_{cat}/(K_{d,Mn}K_{m,Mal}K_{m,NADP})]$ at least four orders of magnitude smaller than the WT value. This difference corresponds to an increase of 6.38 kcal/mol energy barrier for the catalytic efficiency. Mutation at Asp464, on the other hand, has partial additivity on the mutations at Asp141 and Asp194. The overall specificity constants for the double mutants D(194,464)N and D(141,464)N or the triple mutant D(141,194,464)N were decreased by only 10- to 100-fold compared to the WT. These results strongly suggest the involvement of Asp141 in the Mn^{2+}-L-malate binding for the pigeon liver malic enzyme. The Asp194 and Asp464, which may be oxidized by nonspecific binding of Cu^{2+}, are involved in the Mn^{2+}-L-malate binding or catalysis indirectly by modulating the binding affinity of Asp141 with the Mn^{2+}.

Keywords: binding cooperativity; binding energy; enzyme engineering; metal site; site-specific mutagenesis

Reprint requests to: Gu-Gang Chang, Department of Biochemistry, National Defense Medical Center, P.O. Box 90048, Taipei 100, Taiwan, Republic of China; e-mail: ggchang@ndmc1.ndmctsgh.edu.tw.

Abbreviations: D141N, D194N, and D464N, point mutants of the enzyme with asparagine substituted for aspartate at position 141, 194, or 464, respectively; D(141,194)N, D(194,464)N, and D(141,464)N, double mutants of the enzyme with asparagine substituted for aspartate at positions 141 and 194, 194 and 464, or 141 and 464, respectively; D(141,194,464)N, triple mutant of the enzyme with asparagine substituted for aspartate at positions 141, 194, and 464; MCO, metal-catalyzed oxidation; PAGE, polyacrylamide gel electrophoresis; PCR, polymerase chain reaction; SDS, sodium dodecyl sulfate; WT, wild-type pigeon liver malic enzyme.

Malic enzyme [(*S*)-malate:$NADP^+$ oxidoreductase (oxaloacetate-decarboxylating), EC 1.1.1.40] was first discovered in pigeon liver by Ochoa et al. (1947) more than 50 years ago. It was later found widespread in nature, from bacteria to human, and was thus thought to be a housekeeping enzyme. In animals and the human body, the major physiological function of the enzyme is to provide NADPH for the de novo biosynthesis of long-chain fatty acids (Frenkel, 1975; Goodridge et al., 1989).

The enzyme is a bifunctional enzyme catalyzing the divalent metal ion (Mn^{2+} or Mg^{2+}) dependent reversible oxidative decarboxylation of L-malate. The enzymatic reaction proceeds in two

consecutive steps. L-Malate is first oxidized by $NADP^+$ generating an enzyme-bound oxaloacetate, which is then decarboxylated to give CO_2 and pyruvate. Cleland's group (Hermes et al., 1982; Urbauer et al., 1998) and Cook's group (Karsten et al., 1999) have elaborated this stepwise mechanism by using the kinetic isotope effect technique.

In the structure–function relationship studies of pigeon liver malic enzyme, we have demonstrated the importance of Lys2/Lys3, Arg9, and Phe19 at the N-terminus of this enzyme for the Mn^{2+}–L-malate binding and for the subunit association (Chou et al., 1996a, 1996b, 1997, 1998; Huang et al., 1998). The metal binding site of the enzyme was further characterized with metal-catalyzed oxidation (MCO) systems. The oxidation of biomacromolecules by the MCO systems are involved in many physiological and pathological conditions (Stohs & Bagchi, 1995; Jacobson, 1996; Davies & Dean, 1997; Vaughan, 1997 and references therein; Hippeli & Elstner, 1999). Pigeon liver malic enzyme was found to be very sensitive to MCO systems (Wei et al., 1994; Chou et al., 1995). We have successfully used the Fe^{2+}–ascorbate system in characterizing the possible metal-binding site of malic enzyme (Wei et al., 1994), which was affinity cleaved at Asp258. Involvement of Asp258 as the Mn^{2+} binding ligand was further confirmed by site-specific mutagenesis (Wei et al., 1995). The proposal of Asp258 as a direct metal ligand is proven correct by the recently resolved crystal structure of human mitochondrial malic enzyme (Xu et al., 1999).

When the MCO system was changed to Cu^{2+}-ascorbate and at acidic pH, an entirely different cleavage pattern of the enzyme molecule was observed that allowed us to identify Asp141, Asp194, and Asp464 as the other putative Mn^{2+}-binding ligands of the enzyme (Chou et al., 1995). This possibility was further characterized by site-specific mutagenesis in the present investigation. We have provided strong evidence to suggest that Asp141 be involved in the Mn^{2+}–L-malate binding for the pigeon liver malic enzyme. These results provide important information about the metal-binding milieu of malic enzyme and will be useful in redesigning the metal site of malic enzyme for improving its stabilization (Higaki et al., 1992; Regan, 1993; Klemba et al., 1995; Lu & Valentine, 1997; Hellinga, 1998).

Results

Purification and preliminary characterization of the expressed recombinant pigeon liver malic enzymes

The WT and various mutants of malic enzyme were successfully expressed and purified to apparent homogeneity by Q-Sepharose and adenosine-2′,5′-bisphosphate-agarose columns. The WT had an overall recovery of 80% with specific activity of 35 U/mg, which is comparable to the value of the natural pigeon liver malic enzyme (Chang & Chang, 1982). The affinity column was the most effective way to achieve purification of the malic enzyme. For the recombinant malic enzymes, the recovery was usually between 44–88%, with the triple mutant D(141,194,464)N as the only exception, which had an overall yield of only 15%. This is because the triple mutant had very low binding affinity with the adenosine-2′,5′-bisphosphate-agarose affinity column, with the result that it is less satisfactory for the purity of the triple mutant. However, a major protein band corresponding to approximately M_r 65,000, the reported molecular weight of malic enzyme, was observed in the SDS/PAGE for all recombinant malic enzymes (Fig. 1).

All mutant malic enzymes had similar thermal stability to the WT when examined by the 58 °C incubation. Under the native conditions with same protein concentration, the WT and all mutant malic enzymes absorbed ultraviolet light with maximum absorption wavelength at 280 nm, with similar extinction coefficients and emitted fluorescence maximum at 320 nm with the same emission intensity, showing similar conformation for the WT and mutants. Furthermore, because all mutant enzymes have some kinetic properties that are similar to those of the WT (vide infra), those mutant malic enzymes should retain enough structure to bind substrates and perform the catalytic reaction.

Among the point mutants, only D141N showed slower inactivation rate by the Cu^{2+}–ascorbate system at pH 5.0 compared to the WT. After the Cu^{2+}–ascorbate incubation for 2 h, the residual enzyme activity left was 80% for D141N but only 20% for the WT, D194N, or D464N mutants. However, all point mutants were competitively inhibited by Cu^{2+} with respect to Mn^{2+}; albeit the D141N and D194N mutants had larger inhibition constants than the WT,

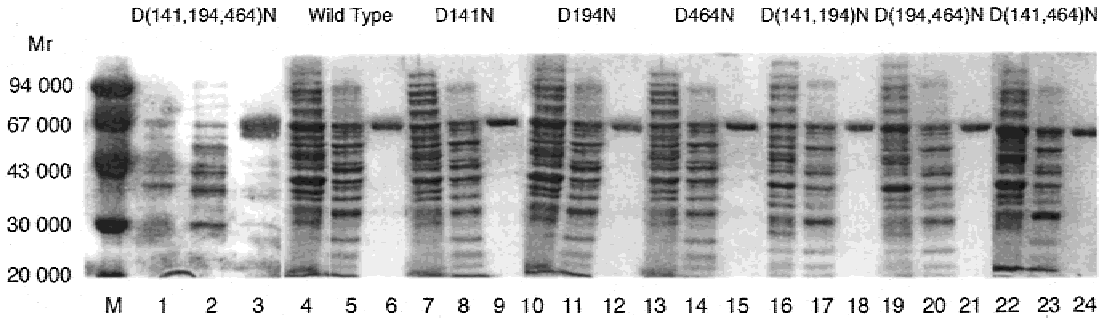

Fig. 1. Polyacrylamide gel electrophoresis in the presence of sodium dodecyl sulfate of the recombinant pigeon liver malic enzymes. The enzyme samples from different purification steps were subjected to SDS/PAGE as described in Materials and methods. Lane M is the M_r standards: phosphorylase *b*, M_r 94,000; bovine serum albumin, M_r 67,000; ovalbumin, M_r 43,000; carbonic anhydrase, M_r 30,000; trypsin inhibitor, M_r 20,000. Lanes 1, 4, 7, 10, 13, 16, 19, and 22 are those of the crude extract (protein amount loaded: 9.6–14 μg/lane). Lanes 2, 5, 8, 11, 14, 17, 20, and 23 are those samples from the Q-Sepharose column (protein amount loaded: 13–17 μg/lane). Lanes 3, 6, 9, 12, 15, 18, 21, and 24 are those from the affinity column (protein amount loaded: 1.8–2.2 μg/lane). Lanes 1–3, D(141,194,464)N triple mutant; lanes 4–6, WT; lanes 7–9, D141N; lanes 10–12, D194N; lanes 13–15, D464N; lanes 16–18, D(141,194)N; lanes 19–21, D(194,464)N; and lanes 22–24, D(141,464)N. The results are composed of different slab gels from different preparations.

indicating their weakening binding affinity with the Cu^{2+}. The inhibition constant ($K_{i,Cu}$) values were 15.4 ± 3.4, 54.7 ± 3.4, 50 ± 2.5, and 11.2 ± 5.3 μM for the WT, D141N, D194N, and D464N, respectively.

Preliminary kinetic analysis indicated that the apparent $K_{m,NADP}$ values for all mutants were similar to the WT value. The triple mutant, which has a low affinity with the adenosine-2′,5′-bisphosphate-agarose affinity column, also showed similar $K_{m,NADP}$ with that of the WT. These results suggest that the structural environment of the nucleotide-binding domain may not be disturbed by the mutations. The $K_{m,Mal}$ and $K_{m,Mn}$, on the other hand, varied considerably among mutants. The strong substrate inhibition by L-malate in WT was only observed in the D464N and D(141,464)N mutants. The detailed kinetic behaviors of these mutants were then analyzed with the initial velocity studies to derive the K_m value for metal ion in the absence of L-malate ($K_{d,Mn}$) and the K_m value for L-malate.

Kinetic properties of the recombinant pigeon liver malic enzymes

All recombinant malic enzymes showed intercepting patterns for the initial velocity experiment (Fig. 2). These results indicate that the sequential kinetic mechanism of the enzyme in the Mn^{2+} and L-malate binding (Hsu et al., 1976; Wei et al., 1995) was not changed after mutation at these putative metal sites. All mutants exhibited a smaller catalytic constant (k_{cat}) than the WT. The $K_{m,Mal}$ for D141N or D194N mutants was increased by 5.2- or 7.3-fold, respectively, compared to the WT value (Table 1). Only the D141N mutant had $K_{m,Mn}$ and $K_{d,Mn}$ values that were increased by approximately 13-fold more than the WT value. Although Asp194 and Asp464 were thought to be located in the metal-binding milieu of the enzyme, because these two residues were cleaved by the Cu^{2+}-ascorbate system (Chou et al., 1995), it turns out that these are not the cases. Mutation of Asp194 or Asp464 alone to asparagine residue does not alter the metal interaction or binding to the enzyme.

Mildvan's group (cf. Kuliopulos et al., 1990) had theoretically and experimentally evaluated the effects of multiple mutations on the kinetic constants of an enzyme. The malic enzyme catalyzed oxidative decarboxylation follows an ordered bi-ter kinetic mechanism (Hsu et al., 1967). For the mutants, an overall specificity constant $[k_{cat}/(K_{d,Mn}K_{m,Mal}K_{m,NADP})]$ is an appropriate kinetic parameter that should reflect the structural perturbations of the environment in the transition state of the central $E\cdot Mn^{2+}\cdot$ L-malate$\cdot NADP^+$ complex. The product of the relative $k_{cat}/(K_{d,Mn}K_{m,Mal}K_{m,NADP})$ values of D141N ($10^{-2.6}$) and D194N ($10^{-1.6}$) is comparable ($10^{-4.2}$) to that of the D(141,194)N double mutant ($10^{-4.6}$). However, this is not the case for the Asp464 mutant. Furthermore, Asp194 and Asp464 seem to play an opposite role in the effect on the binding between Asp141 and Mn^{2+}. We thus applied more rigorous analysis to the interactions between these three aspartate residues by the double mutation cycles and triple mutation box theories (Carter et al., 1984; Fersht et al., 1992; Horovitz & Fersht, 1992; Mildvan et al., 1992).

Interactions between residues Asp141, Asp194, and Asp464 in the pigeon liver malic enzyme

To quantitatively evaluate the interactions of the effects of any mutation on the kinetic binding parameters, the difference in free energy $\Delta(\Delta G)$ by a mutation is estimated by Equation 1, in which the increased free energy $\Delta(\Delta G)$ is expressed as ΔG_{mut}:

$$\Delta G_{mut} = -RT\ln K_{WT} - (-RT\ln K_{mutant}) = RT\ln(K_{mutant}/K_{WT}), \quad (1)$$

where K_{WT} and K_{mutant} are the dissociation or Michaelis constants for the WT and the mutant, respectively. R is the gas constant and T is the absolute temperature.

The contribution of mutation in decreasing the k_{cat} value measures the introduction of energy barrier in catalysis and can be estimated by the following relationship: $\Delta G_{mut} = [RT\ln(k_{cat,mutant}/k_{cat,WT})]$, which will give a negative sign in the calculated value for the cases of elevating activation energy. A positive sign represents decreasing of the activation energy. The effects of mutation on the transition state stabilization, as reflected in the $k_{cat}/(K_{d,Mn}K_{m,Mal}K_{m,NADP})$ values, were calculated in a similar manner as described for k_{cat}. The weakening effect of mutations on the nucleotide and L-malate binding was estimated by evaluating the K_m values (Mildvan et al., 1992).

Double mutants of independent acting residues will give additive effects. Any synergistic or antagonistic interactions between two residues were analyzed by the double mutation cycles as shown in Figure 3. The coupling energy ($\Delta\Delta G_{int}$) between residues A and B in the A/B double mutant was calculated according to Equation 2 (Mildvan et al., 1992):

$$\Delta\Delta G_{int} = \Delta G_{\text{double mutant}} - (\Delta G_{\text{mutant A}} + \Delta G_{\text{mutant B}}) \quad (2)$$

in which $\Delta\Delta G_{int}$ measures the cooperative contribution by both A and B. A positive sign means a synergistic effect exists between A and B, zero for additive effect between A and B, and a negative sign for an antagonistic effect.

The triple mutation box shown in Figure 4 may provide further information concerning the interactions among all three mutating positions (Horovitz & Fersht, 1992).

$$\begin{aligned}\Delta\Delta\Delta G_{int} &= \Delta G_3 - \sum \Delta G_2 + \sum \Delta G_1 \\ &= \Delta G_3 - \sum \Delta\Delta G_{int} - \sum \Delta G_1 \end{aligned} \quad (3)$$

where ΔG_3 is the free energy change for the triple mutant; $\Sigma\Delta G_2$ and $\Sigma\Delta G_1$ are the summation of the free energy changes for all the double mutants and point mutants, respectively. $\Delta\Delta\Delta G_{int}$ measures the cooperativity involved in the three point mutations.

The Gibbs free energy changes involved in different kinetic parameters for all mutants are listed in Table 2. The possible interactions between aspartate residues 141, 194, and 464 are summarized in Table 3. The opposite signs of the calculated values of $\Delta\Delta G_{int(141,194)}$ and $\Delta\Delta G_{int(141,464)}$ in $K_{d,Mn}$ or $K_{m,Mn}$ clearly indicate that opposite interactions exist between Asp141 and Asp194 or Asp141 and Asp464 in the metal binding. The sum of the free energy barriers to Mn^{2+} binding introduced by the single mutants D141N (1.52 kcal/mol) and D194N (0.59 kcal/mol) is 2.11 kcal/mol, which is 1.02 kcal/mol less than that in the D(141,194)N double mutant (3.13 kcal/mol), indicating a synergistic weakening of Mn^{2+} binding in the double mutant. Such synergy indicates anticooperativity in the Mn^{2+} binding by Asp141 and Asp194, in the wild-type enzyme by 1.02 kcal/mol (Mildvan et al., 1992). Thus, Asp194 destabilizes metal binding by Asp141. This is more easily seen by the fact that the D141N mutation is more damaging

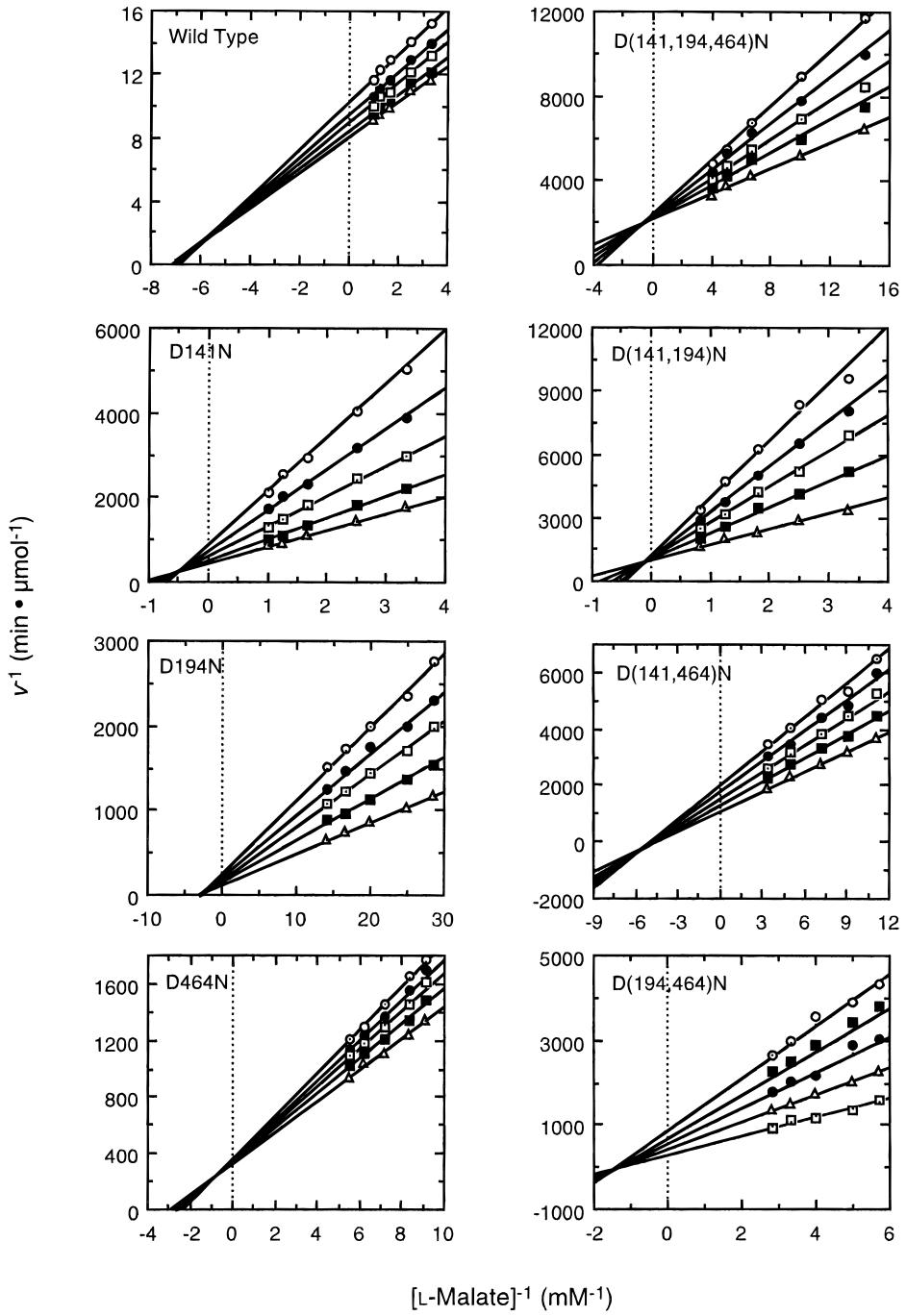

Fig. 2. Initial velocity patterns with respect to L-malate and manganese ion for the recombinant pigeon liver malic enzymes. In WT, from top to bottom, the [Mn^{2+}] was 4.0, 5.0, 8.0, 10, and 15 μM, respectively. For mutants, from top to bottom, the [Mn^{2+}] was 3.0, 4.0, 5.5, 8.0, and 10.5 μM, respectively, in D141N; 2.5, 3.0, 3.5, 4.5, and 6.0 μM, respectively, in D194N; 3.5, 4.0, 4.5, 5.5, and 7.0 μM, respectively, in D464N; 55, 70, 90, 125, and 220 μM, respectively, in D(141,194)N; 5.0, 6.0, 8.0, 11.5, and 20 μM, respectively, in D(194,464)N; 8.6, 10, 12, 15, and 20 μM, respectively, in D(141,464)N; and 13, 16, 20, 26, and 40 μM, respectively, in D(141,194,464)N. The symbols are those of the experimental data. The lines through these data are computer fitting results according to Equation 4.

to metal binding in the presence of D194N (67-fold, Table 1) than in the wild-type (12.3-fold, Table 1).

Conversely, the sum of the free energy barriers to Mn^{2+} binding introduced by D141N (1.52 kcal/mol) and D464N (0.09 kcal/mol) is 1.61 kcal/mol, which exceeds that in the D(141,464)N double mutant (0.91 kcal/mol) by 0.70 kcal/mol, indicating partial additivity of the two effects in the double mutant. Such partial additivity indicates cooperativity between Asp141 and Asp464 in Mn^{2+} binding, by 0.70 kcal/mol. Overall mutation at Asp141, Asp194, and Asp464 destabilize the metal binding of the enzyme by 1.54

Table 1. *Kinetic parameters of the recombinant malic enzymes*

Parameters	WT	D141N	D194N	D464N	D(141,194)N	D(141,464)N	D(194,464)N	D(141,194,464)N
$K_{d,\mathrm{Mn}}$ (μM)[a]	4.4 ± 0.1	54.9 ± 0.5	11.8 ± 2	5.1 ± 0.5	791 ± 80	20 ± 2	32.8 ± 3	54.4 ± 5
$K_{m,\mathrm{Mn}}$ (μM)[a]	1.2 ± 0.2	16.8 ± 2.4	1.5 ± 0.2	1.5 ± 0.1	118 ± 22	12 ± 3	7.7 ± 0.8	10.1 ± 1.4
$K_{m,\mathrm{Mal}}$ (μM)[a]	85.4 ± 15	448 ± 46	623 ± 48	115 ± 11	523 ± 37	120 ± 9	262 ± 19	82.6 ± 7.8
$K_{m,\mathrm{NADP}(app)}$ (μM)	3.8 ± 0.4	6.1 ± 0.7	0.8 ± 0.1	1.9 ± 0.4	10.8 ± 0.8	2.8 ± 0.2	6.6 ± 0.5	2.6 ± 0.2
$K_{i,\mathrm{Mal}(app)}$ (mM)	8 ± 2	367 ± 121	721 ± 327	26 ± 4	482 ± 188	26 ± 3	616 ± 423	164 ± 38
k_{cat} (s^{-1})[a]	369 ± 5	84.3 ± 4	36.8 ± 4	157 ± 1.2	28.3 ± 1	65.1 ± 1.6	105 ± 3.6	91.1 ± 2
$k_{cat}/(K_{d,\mathrm{Mn}}K_{m,\mathrm{Mal}}K_{m,\mathrm{NADP}})$ (μM^{-3} s^{-1})	0.25	5.6×10^{-4}	6.3×10^{-3}	0.14	6.3×10^{-6}	9.7×10^{-3}	1.9×10^{-3}	7.8×10^{-3}
Relative k_{cat}	1.00	0.23	0.10	0.43	0.08	0.18	0.28	0.25
Relative $k_{cat}/(K_{d,\mathrm{Mn}}K_{m,\mathrm{Mal}}K_{m,\mathrm{NADP}})$	1.00	$10^{-2.6}$	$10^{-1.6}$	$10^{-0.25}$	$10^{-4.6}$	$10^{-1.4}$	$10^{-2.1}$	$10^{-1.5}$

[a] These results were obtained from fitting the experimental data to Equation 4.

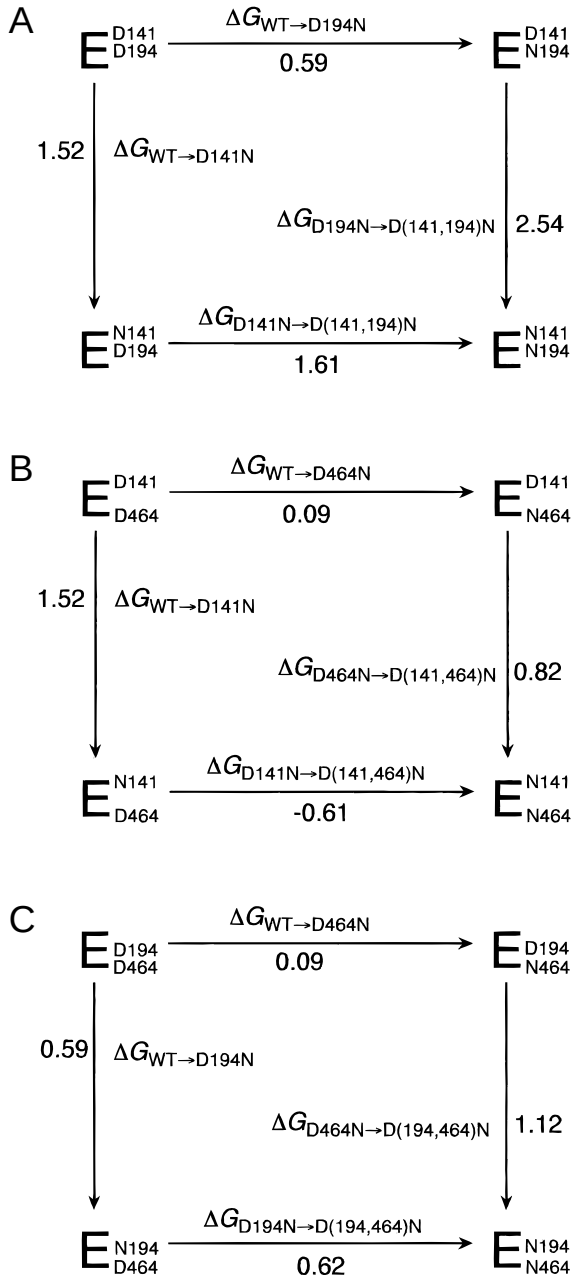

Fig. 3. Double mutation cycles for the D(141,194)N, D(141,464)N, and D(194,464)N double mutants. Thermodynamic double mutant cycles [(**A**) D(141,194)N, (**B**) D(141,464)N, and (**C**) D(194,464)N] show the free energy changes of the WT (upper left edge of the cycles) and the double mutants (bottom right edge of the cycles). The numbers shown in each mutation step represent the free energy change (ΔG_{mut} in kcal/mol) for the metal binding calculated from the $K_{d,\mathrm{Mn}}$ values. A positive value of ΔG_{mut} reflects increasing barrier to Mn^{2+} binding.

kcal/mol indicating a strong interaction between these three aspartate residues in the metal binding milieu of the malic enzyme. Mutation at both the Asp141 and Asp194 has the greatest effect on the overall catalytic efficiency. The value of the overall specificity constant, $k_{cat}/(K_{d,\mathrm{Mn}}K_{m,\mathrm{Mal}}K_{m,\mathrm{NADP}})$, for the D(141,194)N double mutant is at least four orders of magnitude smaller than the WT value, corresponding to an increase of 6.38 kcal/mol energy barrier for the catalytic efficiency.

Table 2. *Thermodynamic parameters for the D(141,194)N, D(141,464)N, and D(194,464)N double mutants and the D(141,194,464)N triple mutant of the recombinant malic enzymes* [a]

	(kcal mol^{-1})						
Parameters	$\Delta G_{WT\rightarrow D141N}$	$\Delta G_{WT\rightarrow D194N}$	$\Delta G_{WT\rightarrow D464N}$	$\Delta G_{WT\rightarrow D(141,194)N}$	$\Delta G_{WT\rightarrow D(141,464)N}$	$\Delta G_{WT\rightarrow D(194,464)N}$	$\Delta G_{WT\rightarrow D(141,194,464)N}$
$K_{d,Mn}$	1.52	0.59	0.09	3.13	0.91	1.21	1.51
$K_{m,Mn}$	1.59	0.13	0.13	2.76	1.39	1.12	1.28
$K_{m,Mal}$	1.0	1.2	0.18	1.09	0.20	0.67	−0.02
$K_{m,NADP}$	0.28	−0.94	−0.42	0.63	−0.18	0.33	−0.23
k_{cat}	−0.9	−1.39	−0.51	−1.55	−1.04	−0.76	−0.84
$k_{cat}/(K_{d,Mn}K_{m,Mal}K_{m,NADP})$	−3.67	−2.22	−0.35	−6.38	−1.96	−2.94	−2.09

[a] Positive ΔG_{mut} values reflect increasing barriers to binding or decreasing of activation energy ($\Delta G^{\ddagger}$) in catalysis.

Table 3. *Calculated thermodynamic parameters for the double-mutation cycles and the triple-mutation box of the recombinant malic enzymes* [a]

	(kcal mol^{-1})					
Parameters	$\Delta G_{D141N\rightarrow D(141,194)N}$	$\Delta G_{D141N\rightarrow D(141,464)N}$	$\Delta G_{D194N\rightarrow D(141,194)N}$	$\Delta G_{D194N\rightarrow D(194,464)N}$	$\Delta G_{D464N\rightarrow D(141,464)N}$	$\Delta G_{D464N\rightarrow D(194,464)N}$
$K_{d,Mn}$	1.61	−0.61	2.54	0.62	0.82	1.12
$K_{m,Mn}$	1.17	−0.20	2.63	0.99	1.26	0.99
$K_{m,Mal}$	0.09	−0.80	−0.11	−0.53	0.02	0.49
$K_{m,NADP}$	0.35	−0.46	1.57	1.27	0.24	0.75
k_{cat}	−0.65	−0.14	−0.16	0.63	−0.53	−0.25
$k_{cat}/(K_{d,Mn}K_{m,Mal}K_{m,NADP})$	−2.71	1.71	−4.16	−0.72	−1.61	−2.59

Parameters	$\Delta G_{D(194.464)N\rightarrow D(141,194,464)N}$	$\Delta G_{D(141,464)N\rightarrow D(141,194,464)N}$	$\Delta G_{D(141.194)N\rightarrow D(141,194,464)N}$	$\Delta\Delta G_{int(141,194)}$	$\Delta\Delta G_{int(141,464)}$	$\Delta\Delta G_{int(194,464)}$	$\Delta\Delta\Delta G_{int(141,194,464)}$
$K_{d,Mn}$	0.30	0.60	−1.62	1.02	−0.70	0.53	−1.54
$K_{m,Mn}$	0.16	−0.11	−1.48	1.04	−0.33	0.86	−2.14
$K_{m,Mal}$	−0.69	−0.22	−1.11	−1.11	−0.98	−0.71	0.40
$K_{m,NADP}$	−0.56	−0.41	−0.86	1.29	−0.04	1.69	−2.09
k_{cat}	−0.08	0.20	0.71	0.74	0.37	1.14	−0.29
$k_{cat}/(K_{d,Mn}K_{m,Mal}K_{m,NADP})$	0.85	−0.13	4.29	−0.49	2.06	−0.37	2.95

[a] Positive ΔG_{mut} values reflect increasing barriers to binding or decreasing of activation energy ($\Delta G^{\ddagger}$) in catalysis.

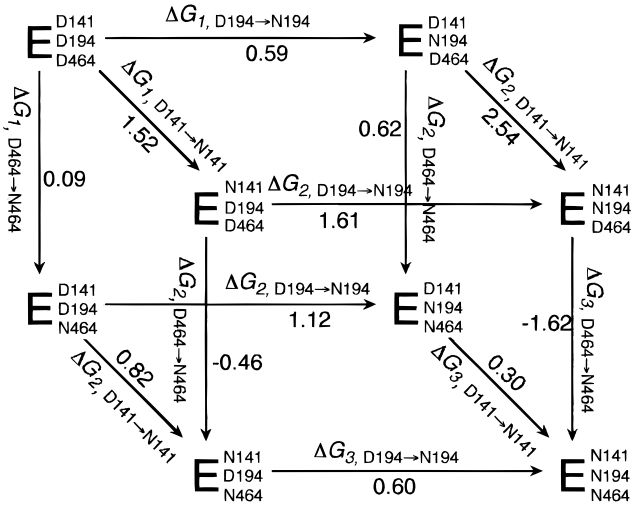

Fig. 4. Triple mutation box for the D(141,194,464)N triple mutant. Thermodynamic triple mutant box shows the free energy changes of the WT (upper left edge of the box) and the triple mutant (bottom right edge of the box). The numbers shown in each mutation step represent the free energy change (ΔG_{mut}, in kcal/mol) for the metal binding calculated from the $K_{d,Mn}$ values. A positive value of ΔG_{mut} reflects increasing barrier to Mn^{2+} binding.

The effect of mutations on the transition state stabilization of the catalytic reaction was also revealed by the k_{cat} changes. Mutation at Asp141, Asp194, and Asp464 decreasing the stability of the transition state by elevating the activation energy ($\Delta G^{\ddagger}$) of 0.9, 1.39, and 0.51 kcal/mol, respectively. The positive values of $\Delta\Delta G_{int}$ (Table 3) for the three double mutants indicate synergistic effects, which suggest that these noninteracting aspartate residues might facilitate the same nonrate–limiting step (Mildvan et al., 1992).

Discussion

For an enzyme that requires metal ion during catalysis, identification of the metal site by metal-catalyzed oxidation has been developed as one of the most powerful techniques in characterizing the metal ligands (Berlett & Stadtman, 1997; Hlavaty & Nowak, 1997; Cao & Barany, 1998; Gallagher et al., 1998). The most promising characteristic of this technique is that the oxidation often occurred as a caged reaction and is accompanied by subsequent affinity cleavage at the putative metal site, which is extremely useful in identifying the putative metal ligands. Usually the cleavage occurs at limited sites, which make separation of the cleaved peptides a simple routine; usually a SDS/PAGE is adequate. Because of advances in protein sequencing technology, blotting of the cleaved peptides from the SDS/PAGE plate into the polyvinylidene difluoride (PVDF) membrane allows sequencing of these peptides to be performed directly in the membrane. This is an obvious advantage over affinity labeling modification that is usually not followed by cleavage. Site-specific proteases are needed to cleave the peptide chain and the subsequent separation of labeled active-site peptide involves the most challenging step for characterizing the labeling site.

The present investigation clearly indicates that metal-catalyzed oxidation and subsequent affinity cleavage, like chemical modification, have some pitfalls that one should be aware of. The oxidation and cleavage sites, even if it happened to be a reasonable metal site, should not be unambiguously taken as the metal-binding ligand. The susceptibility of amino acids toward oxidation and cleavage varies among proteins according to the individual local environment in each case. Oxidation and cleavage sites by the MCO system represent the most susceptible sites in the locally generated free radical environment at the putative metal-binding site, which deserves detailed analysis of its functional role.

It was found that millimolar range of Cu^{2+} actually promoted the oxidative decarboxylation activity of malic enzyme (Rutter & Lardy, 1958), and in the micromolar range, Cu^{2+} is competitively inhibitory against Mn^{2+} in WT (Chou et al., 1995) or mutant enzymes (this study). Cu^{2+} is thus assume to have high affinity with the malic enzyme and compete with Mn^{2+} for the enzyme's metal site that induces a caged modification reaction in the presence of ascorbate (Chou et al., 1995). We, therefore, obtained limited and specific cleavage pattern in the Cu^{2+}-induced oxidative modifications as reported previously (Chou et al., 1995). For confirming these putative metal sites to be the true metal-binding ligands, site-directed mutagenesis was employed. It turns out that although all cleavage sites are the negatively charged aspartate residues, which appear to be excellent ligands for the positively charged metal ion, removing the negative charge by mutating it to the asparagine residue does not always abolish the metal binding. Because a divalent ion Mg^{2+} or Mn^{2+} is absolutely essential for the malic enzyme-catalyzed reaction, any factor influencing the metal binding should be reflected in the k_{cat} or $K_{m,Mn}$ ($K_{d,Mn}$) values. However, the $K_{m,Mn}$($K_{d,Mn}$) values for D194N and D464N are comparable to those of the WT value. These results do not rule out direct involvement of Asp194 or Asp464 as Mn^{2+} binding ligands, but do argue strongly that they probably do not function as such. However, it is also possible for malic enzyme to have a weaker, nonspecific binding of Cu^{2+} at Asp194 and Asp464 that results in oxidative damage in the presence of ascorbate with the induction of redox chemistry as demonstrated previously (Chou et al., 1995). A time-dependent study of the differential rates of cleavage is designed and aimed to delineate this possibility.

The above conclusion is corroborated by the recently solved crystal structure of human mitochondrial malic enzyme (Xu et al., 1999), which has an overall 56% identity and 71% similarity with the pigeon liver malic enzyme. As shown in Figure 5, the functional unit of the enzyme is a dimer. Each monomer is composed of four structural domains with the active site formed from domains A, B, and C (Xu et al., 1999). Asp194 and Asp464, located at domains B and A, respectively, are remote from the active center. On the other hand, Asp141 is located near to the modeled metal ligands Glu234 and Asp235. The corresponding residue of Asp141 in the human mitochondrial malic enzyme is Asp162, which seems not to be involved in metal binding due to improper orientation and distance. Involvement of Glu234, Asp235, and Asp258 in the metal binding has been identified in the crystal structure of the enzyme complex with Yb^{3+} or Lu^{3+} (R. Batra, Z. Yang, D.L. Floyd, H.C. Hung, G. Bhargava, G.G. Chang, L. Tong, unpubl. obs.). However, there might be some subtle structural differences between the pigeon liver cytosolic and human mitochondrial malic enzymes. Alternatively, Asp141 could be involved in the Mn^{2+}-L-malate binding, but not a direct metal ligand. The side chain of Asp141 is located right next to that of Phe236, which directly follows the Mn^{2+} ligands Glu234 and Asp235. A local change in the Asp141 environment, caused by the Asp → Asn mutation, might perturb the conformations of Glu234 and/or Asp235, and thereby have an indirect effect on the Mn^{2+} binding.

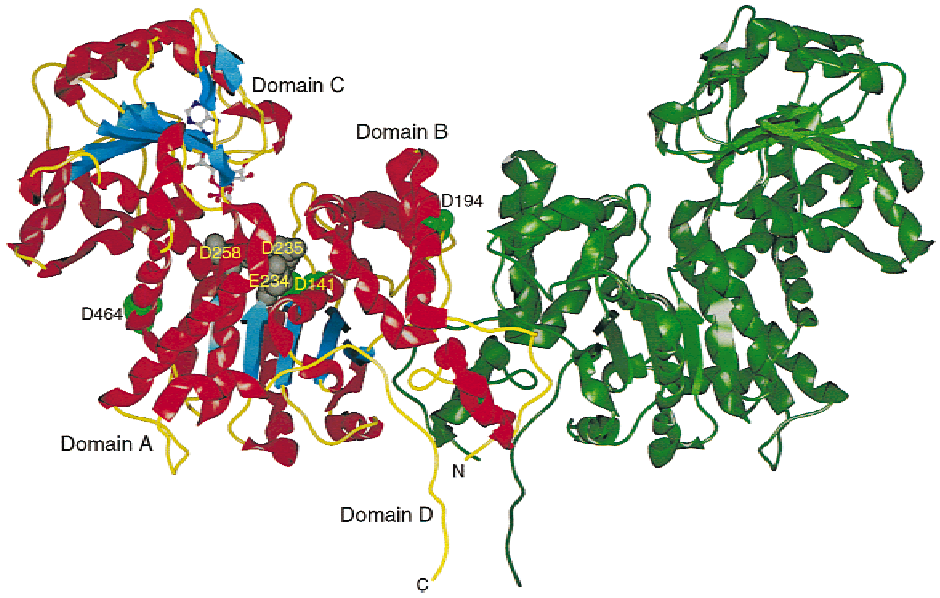

Fig. 5. Crystal structure of the functional dimer of human mitochondrial malic enzyme. Malic enzyme is a tetramer with double dimer structure. The structural features of the enzyme are color coded in one of the subunits, α-helices in red, β-strands in blue, and random coil in yellow. Each subunit composes of four structural domains (**A**–**D**). The metal ligands Glu234, Asp235, and Asp258 are highlighted with space-filling representation in gray. The mutation positions in this study are shown in space-filling representation in green. The numbering system of the amino acid residues is that for the pigeon liver malic enzyme. The corresponding numbers in the human mitochondrial enzyme are Glu255, Asp256, and Asp279, respectively. The bound nucleotide at domain C is shown with ball-and-stick representation in CPK color. N and C denote the amino- and carboxyl-termini of the polypeptide chain, respectively. The other subunit is shown in green.

Direct evidence for the participation of Asp141 in the metal binding of pigeon liver malic enzyme will be awaited for the crystal structure of the cytosolic enzyme to elucidate.

Manganous ion, via metal-bound water molecules, participates in polarization of the carbonyl and carboxyl groups of the dianion transition state, which is located at the second sphere of the metal ion (Hsu et al., 1976). We have identified Asp258 of the enzyme molecule as a direct binding ligand by the techniques of metal-catalyzed oxidation and site-directed mutagenesis (Wei et al., 1994, 1995) and by structural work (Xu et al., 1999). In the present paper, we show that the $K_{m,\mathrm{NADP}}$ was not appreciably altered for all the mutants we studied, indicating that all these mutations are not involved in the nucleotide binding domain, and domain C of the enzyme is not touched (Fig. 5). On the other hand, mutations at Asp141, Asp194, or Asp464 have different effects on the Mn^{2+}-L-malate binding that result in greatly decreased catalytic efficiency of the enzyme. We have suggested different stability of the Mn^{2+}-L-malate domain and the nucleotide domain, which resulted in a three-state unfolding process of the enzyme upon urea denaturation (Huang et al., 1998). The present results strongly support the location of Asp141 in the Mn^{2+}-L-malate domain. Our results are also corroborated by the early proton relaxation data, which indicate that L-malate or pyruvate, but not the $NADP^+$, interacts with the enzyme-bound Mn^{2+} to decrease the number of fast exchanging water ligands (Hsu et al., 1976).

One of the novel observations reported in this paper is that interactions exist between different aspartate residues in the remote areas of the malic enzyme. The synergistic interactions between Asp141 and Asp194 in the Mn^{2+} binding are clearly shown in the $K_{m,\mathrm{Mn}}$ and $K_{d,\mathrm{Mn}}$ values. Removing the negative charge from Asp141 decreases the Mn^{2+} affinity by an order of magnitude. Mutation at residue 194 itself does not affect the metal binding. However, mutation at both Asp141 and Asp194 reduces the metal binding affinity by another order of magnitude compared with D141N. No interacting was observed between Asp141 and Asp194 in the L-malate binding. The Asp464, however, seems to somewhat offset the binding energy between L-malate and the enzyme contributed from the other two aspartate residues.

The structural basis for the modulatory effects of remote Asp192 and Asp464 on the Mn^{2+} binding is not clear at the present stage. Our mutagenesis data for D464N have essentially ruled out any functional role of Asp464 in the enzyme. D464N has almost the same kinetic parameters as the WT; only $K_{i,\mathrm{Mal}}$ deviates by approximately threefold. Asp464 should have no impact on the catalysis by the enzyme. Like Asp464, Asp194 is also fully exposed on the surface of the enzyme and is far from the active site (Fig. 5). One would expect minimal effects for the D194N mutant. However, the kinetic properties of D194N are dramatically different from those of the WT, approximately sevenfold for $K_{m,\mathrm{Mal}}$, 1/5 for $K_{m,\mathrm{NADP}}$, and 1/10 for k_{cat}. Only the $K_{m,\mathrm{Mn}}$ is comparable to that of the WT. There is no structural reason for these observations. It might be that D194N mutant has some problems with the folding and/or oligomerization. The side chain of Asp194 is in the vicinity of the dimer interface (Fig. 5). Our previous experimental results indicated that some N-terminal deletion or substitution mutants induced dissociation of the quaternary structure (Chou et al., 1997). The possible effect of mutation at Asp194 on the subunit interactions is now under investigation in this laboratory.

Because Asp141 and Asp258 are highly conserved among malic enzyme from various sources (cf. Wei et al., 1994; Chou et al.,

1995), we conclude that, in the metal-binding milieu of the malic enzyme active center, Asp258, at the metal binding motif of FNDD[258]IQGTA (Wei et al., 1994, 1995), are direct metal binding ligands. Asp141 at the metal binding motif of V(C)VTD[141]GE RILGLGDLG (Chou et al., 1995), may be in the second sphere of the metal site, located near the L-malate binding domain and is indirectly involved in the metal binding (Hsu et al., 1976). The highly conserved Asp194 and the less conserved Asp464 may cooperate in the metal binding in the native pigeon malic enzyme and is the site that may be considered as the future candidate in engineering the metal binding domain of the malic enzyme.

Our results also indicate that the metal binding milieu of proteins is in a balance of many contributing factors. Some of these factors favor the binding, some destabilize it. Adjusting the cooperativity between residues should be taken into consideration in any designing of the metal binding site of proteins.

Materials and methods

Site-specific mutagenesis

Site-directed mutagenesis of point mutants was carried out according to the procedure of Zoller and Smith (1982). The synthetic oligonucleotides used as mutagenic primers were:

D141N, 5′TGTGGTGACA**A**A**C**GGAGAACGCA3′;

D194N, 5′TTTGCTGAAA**A**ACCCTTTGTA3′;

D464N, 5′ACATATTGGC**A**ACGACGTATT3′,

in which the mutation positions were highlighted and underlined in the oligonucleotide sequence. The uracil-containing template DNA was annealed with phosphorylated mutagenic oligonucleotide and in vitro extended by T4 DNA polymerase and T4 DNA ligase, respectively. Restriction enzyme digestion and ligation were used to construct double and triple mutants. A DNA fragment containing the D464N mutation, generating by the *Nsi* I and *Bsu36* I digestions, was used for D(141,464)N and D(194,464)N construction. *Afl* II and *Bsu36* I fragments were used for preparation of D(141,194)N double mutant and D(141,194,464)N triple mutant. The expressed malic enzyme contained an extra Met-Asp-Ser tripeptide at the N-terminus. Except for this small difference, the recombinant wild-type malic enzyme had an otherwise identical amino acid sequence to the natural pigeon liver malic enzyme in the total of 557 amino acid residues. All the mutated cDNAs were also examined by dideoxy chain termination sequencing (Sanger et al., 1977) to exclude any unexpected mutations having resulted from the in vitro extension. The absence of adventitious base changes was verified.

Expression, purification, and spectroscopic analysis of the recombinant pigeon liver malic enzymes

The mutated plasmids were transformed into BL21 bacteria. The transformants were incubated in LB medium and induced by 1 mM isopropyl β-D-thiogalactopyranoside (IPTG). The cells were then harvested by centrifugation at 5,000 $\times$ *g* for 5 min. After sonication, the recombinant enzymes were purified by two successive chromatographic steps, Q-Sepharose and adenosine-2′,5′-bisphosphate-agarose, according to Chang et al. (1991). All purified enzymes were subjected to sodium dodecyl sulfate-polyacrylamide gel electrophoresis (SDS/PAGE) to examine the purity (Chang et al., 1994).

Fluorescence spectra of the recombinant malic enzymes were analyzed with a Perkin-Elmer LS 50B luminescence spectrometer at 30 °C. All spectra were corrected for the buffer absorption. The Raman spectrum of water was also corrected.

Enzyme assay and protein determination

Malic enzyme activity was assayed in triethanolamine-HCl buffer (66.7 mM, pH 7.4) at 30 °C according to the published procedure and the chelations of metal ion by L-malate and $NADP^+$ were corrected (Chang et al., 1992). An enzyme unit was defined as the enzyme amount that catalyzes the production of 1 μmol of NADPH per minute under the assay conditions using an absorption coefficient of 6,220 M^{-1} for the NADPH. Protein concentration was determined by the protein-dye binding method of Bradford (1976). An M_r of 260,000 for the tetrameric enzyme was used in the calculation of k_{cat} values.

Apparent Michaelis constants for the substrate and cofactors were determined by varying the concentration of one substrate (or cofactors) around its K_m value and maintaining the other components constant. Fitting of kinetic data was carried out with the EZ-FIT computer program (Perrella, 1988).

Heat stability

The sensitivity of WT and various mutants of malic enzyme to thermal denaturation were examined by heating the enzyme solution at 58 °C. Aliquots of the sample were redrawn at various time intervals and immediately assayed for enzyme activity. The residual enzyme activity was plotted vs. incubation time, which was fitted to a double exponential equation according to a three-state unfolding model as described previously (Huang et al., 1998).

Enzyme inactivation with the Cu^{2+}–ascorbate system

The inactivation experiments were performed at 0 °C by adding freshly prepared solutions of cupric nitrate (6 μM) and ascorbate (20 mM) into the enzyme solution (0.97 μM) in a sodium acetate buffer (66.5 mM, pH 5.0). The progress of enzyme inactivation was monitored by assaying the residual enzyme activity left in the small aliquots withdrawn at the designated time intervals (Chou et al., 1995).

Initial velocity studies

Initial velocity study was performed by varying the concentration of Mn^{2+} from 3.0 to 10.5 μM and of L-malate concentrations from 0.3 to 1.0 mM. For mutants that have altered metal or L-malate binding affinity, the Mn^{2+} or L-malate concentration was adjusted accordingly. Concentrations of the other components (66.7 mM triethanolamine-HCl buffer, pH 7.4; and 0.23 mM $NADP^+$) were held constant. The enzyme amount used was small enough to give a linear $A_{340\ nm}$ vs. time plot for at least 3–5 min. The slope of this initial recorder tracing was taken as the observed enzyme velocity (v). The data were fitted to Equation 4 with the EZ-FIT computer program (Perrella, 1988) to estimate the various kinetic parameters.

$$v = \frac{V_m[\mathrm{Mal}][\mathrm{Mn}^{2+}]}{K_{d,\mathrm{Mn}}K_{m,\mathrm{Mal}} + K_{m,\mathrm{Mn}}[\mathrm{Mal}] + K_{m,\mathrm{Mal}}[\mathrm{Mn}^{2+}] + [\mathrm{Mal}][\mathrm{Mn}^{2+}]} \quad (4)$$

in which v and V_m are the observed and maximum velocities, respectively. $K_{d,Mn}$, $K_{m,Mn}$, and $K_{m,Mal}$ are the K_m of free Mn^{2+}, extrapolated to zero L-malate concentration, the Michaelis constant for Mn^{2+}, and the Michaelis constant for L-malate, respectively.

Acknowledgments

This work was supported by the National Science Council, Republic of China (Frontier Science Grant NSC 87-2331-B016-008). This paper is derived from the theses presented by H.P. Chang and C.H. Huang in partial fulfillment of the requirements for their MS degrees (Biochemistry), National Defense Medical Center, Taipei, and was presented at the 13th Symposium of the Protein Society held at Boston, Massachusetts, on July 24–28, 1999.

References

Berlett BS, Stadtman ER. 1997. Protein oxidation in aging, disease, and oxidative stress. *J Biol Chem 272*:20313–20316.

Bradford MM. 1976. A rapid and sensitive method for the quantitation of microgram quantities of protein, utilizing the principle of protein-dye binding. *Anal Biochem 72*:248–254.

Cao W, Barany F. 1998. Identification of *Taq*I endonuclease active site residues by Fe^{2+}-mediated oxidative cleavage. *J Biol Chem 273*:33002–33010.

Carter PJ, Winter G, Wilkinson AJ, Fersht AR. 1984. The use of double mutants to detect structural changes in the active site of the tyrosyl-tRNA synthetase (*Bacillus stearothermophilus*). *Cell 38*:835–840.

Chang CT, Chang GG. 1982. Purification of pigeon liver malic enzyme by affinity chromatography. *Anal Biochem 121*:366–369.

Chang GG, Huang TM, Huang SM, Chou WY. 1994. Dissociation of pigeon liver malic enzyme in reverse micelles. *Eur J Biochem 225*:1021–1027.

Chang GG, Huang TM, Wang JK, Lee HJ, Chou WY, Meng CL. 1992. Kinetic mechanism of the cytosolic malic enzyme from human breast cancer cell line. *Arch Biochem Biophys 296*:468–473.

Chang GG, Wang JK, Huang TM, Lee HJ, Chou WY, Meng CL. 1991. Purification and characterization of cytosolic $NADP^+$-dependent malic enzyme from human breast cancer cell line. *Eur J Biochem 202*:681–688.

Chou WY, Huang SM, Chang GG. 1996a. Non-identity of human breast cancer cell cytosolic malic enzyme to that from the normal human cell. *J Protein Chem 15*:273–279.

Chou WY, Huang SM, Chang GG. 1997. Functional roles of the N-terminal amino acid residues in the Mn(II)-L-malate binding and subunit interactions of pigeon liver malic enzyme. *Protein Eng 10*:1205–1211.

Chou WY, Huang SM, Chang GG. 1998. Conformational stability of the N-terminal amino acid residues mutated recombinant pigeon liver malic enzymes. *Protein Eng 11*:371–376.

Chou WY, Liu MY, Huang SM, Chang GG. 1996b. Involvement of Phe^{19} in the Mn^{2+}-L-malate binding and subunit interactions of pigeon liver malic enzyme. *Biochemistry 35*:9873–9879.

Chou WY, Tsai WP, Lin CC, Chang GG. 1995. Selective oxidative modification and affinity cleavage of pigeon liver malic enzyme by the Cu^{2+}-ascorbate system. *J Biol Chem 270*:25935–25941.

Davies MJ, Dean RT. 1997. *Radical-mediated protein oxidation: From chemistry to medicine*. New York: Oxford University Press.

Fersht AR, Matouschek A, Serrano L. 1992. The folding of an enzyme. I. Theory of protein engineering analysis of stability and pathway of protein folding. *J Mol Biol 224*:771–782.

Frenkel R. 1975. Regulation and physiological function of malic enzyme. *Curr Top Cell Regul 9*:157–181.

Gallagher J, Zelenko O, Walts AD, Sigman DS. 1998. Protease activity of 1,10-phenanthroline-copper(I). Targeted scission of the catalytic site of carbonic anhydrase. *Biochemistry 37*:2096–2104.

Goodridge AG, Crish JF, Hillgartmer FB, Wilson SB. 1989. Nutritional and hormonal regulation of the gene for avian malic enzyme. *J Nutr 119*:299–308.

Hellinga HW. 1998. The construction of metal centers in proteins by rational design. *Fold Des 3*:R1–R8.

Hermes JD, Roeske CA, O'Leary MH, Cleland WW. 1982. Use of multiple isotope effects to determine enzyme mechanism and intrinsic isotope effects. Malic enzyme and glucose-6-phosphate dehydrogenase. *Biochemistry 21*:5106–5114.

Higaki JN, Fletterick RJ, Craik CS. 1992. Engineered metalloregulation in enzymes. *Trends Biochem Sci 17*:100–104.

Hippeli S, Elstner EF. 1999. Transition metal ion-catalyzed oxygen activation during pathogenic processes. *FEBS Lett 443*:1–7.

Hlavaty JJ, Nowak T. 1997. Affinity cleavage at the metal-binding site of phosphoenolpyruvate carboxykinase. *Biochemistry 36*:15514–15525.

Horovitz A, Fersht A. 1992. Co-operative interactions during protein folding. *J Mol Biol 224*:733–740.

Hsu RY, Lardy HA, Cleland WW. 1967. Pigeon liver malic enzyme. V. Kinetic studies. *J Biol Chem 242*:5315–5322.

Hsu RY, Mildvan AS, Chang GG, Fung CH. 1976. Mechanism of pigeon liver malic enzyme. Magnetic resonance and kinetic studies of the role of Mn^{2+}. *J Biol Chem 251*:6574–6583.

Huang SM, Chou WY, Lin SI, Chang GG. 1998. Engineering of a stable mutant malic enzyme by introducing an extra ion-pair to the protein. *Proteins 31*:61–73.

Jacobson MD. 1996. Reactive oxygen species and programmed cell death. *Trends Biochem Sci 21*:83–86.

Karsten WE, Hwang CC, Cook PF. 1999. Secondary tritium kinetic isotope effects indicate hydrogen tunneling and coupled motion occur in the oxidation of L-malate by NAD-malic enzyme. *Biochemistry 38*:4398–4402.

Klemba M, Gardner KH, Marino S, Clarke ND, Regan L. 1995. Novel metal-binding proteins by design. *Nat Struct Biol 2*:368–373.

Kuliopulos A, Talalay P, Mildvan AS. 1990. Combined effects of two mutations of catalytic residues on the ketosteroid isomerase reaction. *Biochemistry 29*:10271–10280.

Lu Y, Valentine JS. 1997. Engineering metal-binding sites in proteins. *Curr Opin Struct Biol 7*:495–500.

Mildvan AS, Weber DJ, Kuliopulos A. 1992. Quantitative interpretations of double mutations of enzymes. *Arch Biochem Biophys 294*:327–340.

Ochoa S, Mehler A, Kornberg A. 1947. Reversible oxidative decarboxylation of malic acid. *J Biol Chem 167*:871–872.

Perrella FW. 1988. EZ-FIT: A practical curve-fitting microcomputer program for the analysis of enzyme kinetic data on IBM-PC compatible computers. *Anal Biochem 174*:437–447.

Regan L. 1993. The design of metal-binding sites in proteins. *Annu Rev Biophys Biomed Struct 22*:257–281.

Rutter WJ, Lardy HA. 1958. Purification and properties of pigeon liver malic enzyme. *J Biol Chem 233*:374–382.

Sanger F, Nicklen S, Conlson AR. 1977. DNA sequencing with chain-terminating inhibitors. *Proc Natl Acad Sci USA 74*:5463–5467.

Stohs SJ, Bagchi D. 1995. Oxidative mechanisms in the toxicity of metal ions. *Free Radic Biol Med 18*:321–336.

Urbauer JL, Bradshaw DE, Cleland WW. 1998. Determination of the kinetic and chemical mechanism of malic enzyme using *(2R,3R)-erythro*-fluoromalate as a slow alternate substrate. *Biochemistry 37*:18026–18031.

Vaughan M. 1997. Oxidative modification of macromolecules mini-review series. *J Biol Chem 272*:18513.

Wei CH, Chou WY, Chang GG. 1995. Identification of Asp^{258} as the metal coordinate of pigeon liver malic enzyme by site-specific mutagenesis. *Biochemistry 34*:7949–7954.

Wei CH, Chou WY, Huang SM, Lin CC, Chang GG. 1994. Affinity cleavage at the putative metal binding site of pigeon liver malic enzyme by Fe^{2+}-ascorbate system. *Biochemistry 33*:7931–7936.

Xu Y, Bhargava G, Wu H, Loeber G, Tong L. 1999. Crystal structure of human mitochondrial $NAD(P)^+$-dependent malic enzyme: A new class of oxidative decarboxylases. *Structure 7*:877–889.

Zoller MJ, Smith M. 1982. Oligonucleotide-directed mutagenesis using M13-derived vectors: An efficient and general procedure for the production of point mutations in any fragment of DNA. *Nucleic Acid Res 10*:6487–6500.